Utilization of ferric groundwater treatment residuals for inorganic-organic hybrid biosorbent preparation and its use for vanadium removal

Ruichi Zhang, Tiina Leiviskä, Juha Tanskanen, Baoyu Gao, Qinyan Yue

PII: S1385-8947(18)32608-1
DOI: https://doi.org/10.1016/j.cej.2018.12.122
Reference: CEJ 20662

To appear in: *Chemical Engineering Journal*

Received Date: 31 October 2018
Revised Date: 18 December 2018
Accepted Date: 20 December 2018

Please cite this article as: R. Zhang, T. Leiviskä, J. Tanskanen, B. Gao, Q. Yue, Utilization of ferric groundwater treatment residuals for inorganic-organic hybrid biosorbent preparation and its use for vanadium removal, *Chemical Engineering Journal* (2018), doi: https://doi.org/10.1016/j.cej.2018.12.122

Utilization of ferric groundwater treatment residuals for inorganic-organic hybrid biosorbent preparation and its use for vanadium removal

Ruichi Zhang[a]*, Tiina Leiviskä[a], Juha Tanskanen[a], Baoyu Gao[b], Qinyan Yue[b]

[a]Chemical Process Engineering, P.O. Box 4300, FIN-90014 University of Oulu, Oulu, Finland.

[b]Shandong Provincial Key Laboratory of Water Pollution Control and Resource Reuse, School of Environmental Science and Engineering, Shandong University, Qingdao 266237, China

E-mail: ruichi.zhang@oulu.fi (R. Zhang), tiina.leiviska@oulu.fi (T. Leiviskä), juha.tanskanen@oulu.fi (J. Tanskanen), bygao@sdu.edu.cn (B. Gao), qyyue@sdu.edu.cn (Q. Yue).

Corresponding author: Ruichi Zhang (ruichi.zhang@oulu.fi)

Declarations of interest: none.

Abstract

Ferric groundwater treatment residual (Fe-GWTR) collected from a Finnish groundwater treatment plant were recovered for use after acid dissolution as an iron source for an inorganic-organic hybrid material. Acid dissolution, performed with 1 mol/L hydrochloric acid and mixing for one hour at room temperature, was determined as the optimal condition based on a high Fe concentration and low concentration of interfering elements. Peat modification was conducted at pH values of 3, 5 and 7 with both a commercial iron reagent ($FeCl_3 \cdot 6H_2O$) and Fe-GWTR solution for comparison. A modification pH of 3 resulted in the highest vanadium removal efficiency for both iron sources. The isoelectric point (pH_{IEP}) of Fe-GWTR-modified peat at pH 3 (Fe-GWTR-P3) was found to be 5.0. After modification, it was confirmed that BET surface area and pore volume of the peat were enlarged. Maximum capacity was found to be around 16 mg/g with a 24-hour contact time at pH 4 and a good fit was achieved with the Redlich-Peterson isotherm model. The kinetic data followed the Elovich equation, which refers to the chemisorption mechanism. According to intra-particle

diffusion and Boyd models, the adsorption was a two-step diffusion process, with intra-particle diffusion being the slowest step. This study demonstrates that Fe-GWTR could safely be used as an iron source for biomass modification, and Fe-GWTR-P3 could be used as a low-cost and effective sorbent for vanadium-containing wastewater treatment.

Keywords: Groundwater treatment residual; recover; iron impregnation; vanadium removal.

1. Introduction

In order to utilize more waste materials and support sustainability, recent research has focused extensively on water treatment residuals (WTRs) as one cost-effective material for decreasing/removing various toxic compounds from wastewater. WTRs are non-hazardous waste materials resulting from the coagulation processes of surface waters or oxidation of groundwater containing dissolved iron/manganese [1]. WTRs originating from coagulation are mainly composed of Al and Fe metal (hydr)oxides although they contain some organic polymers, sediment and humic substances [2,3]. Aluminium and iron salts are commonly used as coagulating agents in water treatment, producing Al-WTRs and Fe-WTRs, respectively [3]. At groundwater treatment plants, dissolved iron and manganese in groundwater are oxidized and thus form an insoluble precipitate (referred to as groundwater treatment residual, GWTR). WTRs and GWTRs have great potential for use in water purification due to their large surface area and high reactivity [4,5].

In previous studies, WTRs have been directly used as adsorbents and adsorption behaviour for different types of toxic compounds on WTRs has been widely investigated. Generally, the WTRs were dried, ground and sieved prior to use for adsorption. In these studies, WTRs have been reported to successfully remove trace metal cations such as Cu(II), Pb(II), Cd(II), Zn(II), Co(II), Hg(II), Se(VI), Se(IV) [2,5,6,7,8] and anionic pollutants such as arsenic [5,9], phosphate [10,11]

and chromium [12]. Sorption of boron [13], organophosphate pesticides [14] and hydrogen sulphide [15] onto WTRs has also been studied previously.

Instead of using WTRs directly as an adsorbent, Soleimanifar et al. synthesized and tested wood mulches coated with WTRs for stormwater treatment [16]. The mulch surface was coated with dried WTR powder by means of an environment-friendly mulch glue. Wang et al. applied a sequential thermal and acid activation method on WTRs to improve phosphorus adsorption [17]. Oxygen-limited heat treatment was also used by Wang et al. to improve the adsorptive properties of WTRs [18]. The findings indicated that the sorption capacity was enhanced after the treatment.

To the best of our knowledge, none of the studies have reported the optimization of WTR dissolution and its use as an iron source for sorbents. In this study, the dissolution conditions of ferric groundwater treatment residual Fe-GWTR (hydrochloric acid concentration and mixing time) were optimized by considering the impurities of the Fe-GWTR solution. The feasibility of reusing Fe-GWTR to replace commercial Fe in biomass modification process was to be confirmed in the study. GWTR was collected from the groundwater treatment plant, and thus the iron originated from the groundwater and was removed in the presence of oxygen. Peat was chosen as the support material thanks to its reactivity and availability. Peat, an accumulation of partially decayed vegetation or organic matter, is formed as the first stage of coal formation. It is widely available in a waterlogged environment [19]. Peat contains lignin, cellulose and humic substances as major constituents. These constituents have numerous functional groups, such as alcohols, aldehydes, carboxylic acids, ethers, ketones and phenolic hydroxides [19], which can react with ions in wastewater and are available for chemical modification. Natural peat has been reported to be unsuitable for direct use in the water treatment process because of its poor physical properties and chemical stability [19]. Hence, various modification methods have been investigated with the purpose of improving the sorption ability of natural peat regarding various pollutants. Among these

different modification methods, metal impregnation has been found to be an easy and effective way to increase the adsorption capacity of virgin biomass towards anions [20,21].

Regarding the use of peat as adsorbent, most of the studies have only focused on the removal of metal cations onto peat. However, very little is known about the sorption of vanadium on modified peat. Vanadium exists mostly as cationic forms when pH < 3, while anionic forms dominate when pH > 3 [22]. Vanadium is widely used as a catalyst, pigment, photographic developer, in drying agents etc. in various industries such as the ceramic, glass, textile, photography, metallurgy, rubber and chemical production industries [23]. These industries inevitably generate a lot of vanadium wastewater and the discharge of vanadium-containing wastewater has raised concern in recent years.

This paper presents a novel approach to utilize Fe-GWTR in the modification of peat by optimizing its dissolution into acid and then using the dissolved iron for the modification. The modification process was compared by using both Fe-GWTR solution and commercial Fe ($FeCl_3 \cdot 6H_2O$) as the iron source and the optimal modification pH was also investigated. Batch tests were conducted with synthetic vanadium solution to investigate the effect of aqueous pH and contact time on vanadium sorption, and the maximum capacity. The kinetic data and isotherm data were fitted to different models. X-ray diffraction (XRD), X-ray photoelectron spectroscopy (XPS), Fourier-transform infrared spectroscopy (FTIR), analyses of Brunauer-Emmett-Teller (BET) surface area, pore size distribution and zeta potential were performed to study the properties of the modified peat.

2. Materials and methods

2.1 Raw materials and chemicals

Natural peat was obtained from Stora Enso Veitsiluoto pulp mill in Kemi, northern Finland. The received peat was dried at 80 °C for 24 h and then sieved to obtain the fraction of 90-250 µm. Fe-GWTR was collected from a Finnish groundwater treatment plant treating iron- and manganese-containing water, where Fe-GWTR was formed during the water aeration process. Fe-GWTR was

first dried at 40 °C for 72 hours. Next the dried Fe-GWTR was ground using a hand mortar. Commercial Fe solution was prepared by dissolving $FeCl_3 \cdot 6H_2O$ (Merck) in pure Milli-Q water (Merck Millipore). 1 M and 2 M HCl solutions were prepared from concentrated HCl (Merck). The pH of the commercial Fe and Fe-GWTR solutions was adjusted using NaOH (Sigma-Aldrich). Vanadium concentration was analysed by both phosphorus-tungsten-vanadium acid spectrophotometry [24] (UV-1800, Shimadzu) and inductively coupled plasma optical emission spectrometry (ICP-OES) (Thermo Fisher Scientific ICAP RQ). The results of the two analysis methods were compared for the effect of contact time. The Pearson correlation coefficient was calculated to be 0.995, which confirmed that the phosphorus-tungsten-vanadium acid spectrophotometry method can be trusted for vanadium measurement.

2.2 Dissolution of Fe-GWTR and characterization of Fe-GWTR solution

The dissolution procedure was as follows: 4 g of ground Fe-GWTR particles were dissolved in 200 mL of 1 M or 2 M HCl solution and mixed for 1 hour or 6 hours at room temperature. The water extracts were recovered by two-stage filtration. Firstly, the solution was passed through a funnel with filter paper (Whatman, Grade 1), and then the filtered water extract was filtered with a 0.45 µm membrane (VWR, polyethersulfone membrane). The filtered Fe-GWTR solutions were sent to a certified laboratory for the following analyses: Al, As, B, Ba, Be, Ca, Cd, Co, Cr, Cu, K, Mg, Mo, Mn, Na, Ni, Fe, P, Pb, S, Sb, Se, Si, Sn, V, Zn and Ti, which were analysed using inductively coupled plasma mass spectrometry (ICP-MS) (Thermo Fisher Scientific ICAP RQ) according to standardized methods SFS-EN ISO 17294-2:2005 and SFS-EN ISO 11885:2009.

2.3 Synthesis of the biosorbent and batch sorption test

Raw peat was modified by mixing with commercial Fe solution or Fe-GWTR solution, at an initial Fe concentration of 0.07 M. The optimal modification pH (3, 5 and 7) was studied. Vanadium removal efficiency was chosen as the response. Two repeats were conducted for each iron solution under the same modification pH. Iron-impregnated peat was synthesized as follows: 1 g peat was mixed with 50 mL of 0.07 M Fe solution, and the pH of the Fe solution was adjusted to the desired value (3, 5 or 7) by adding NaOH. The mixture was then stirred with magnetic stirring at room temperature (20±3˚C) for 6 hours. After that, the mixture was transferred to centrifuge beakers for washing with deionized water until the supernatant became colourless and the pH reached neutral. Then the washed modified peat was separated from the solution and dried at 60 ˚C for 24 hours.

Vanadium sorption experiments with raw and modified peat (2 g/L) were carried out in batch mode. Samples were weighed (0.1 g) and transferred into a plastic bottle containing 50 mL of vanadium solution (20 mg/L V) at an initial pH of 5-6 (without pH adjustment). The batch experiments were performed in duplicate for each sample. The bottles were then shaken for 24 h at room temperature on a rotary shaking device (20 rpm). Samples were centrifuged (10 mins, 2500 rpm) and filtered by syringe with a 0.45 µm filter membrane (VWR, polyethersulfone membrane) after batch shaking, then analysed for residual vanadium content. Fe-GWTR-modified peat at pH 3 (referred to as Fe-GWTR-P3) was selected for further study based on the results. Commercial Fe-modified peat at pH 3 (referred to as Comm-Fe-P3) was also chosen for XRD analysis.

2.4 Biosorbent characterization

Porosity analysis for raw peat and Fe-GWTR-P3 was performed by N_2 adsorption and desorption experiments at 77K (JW-BK 122W, Beijing JWGB Sci. & Tech. Co., Ltd, China). The specific surface was calculated by Brunauer-Emmett-Teller (BET). The pore volume was estimated by the

adsorption amount of nitrogen at a relative pressure of 0.99. Barrett-Joyner-Halenda (BJH) method was used to measure pore size distribution

Raw peat, Fe-GWTR-P3 and Comm-Fe-P3 were ground to a fine powder with a hand mortar for characterization by XRD using a Rigaku Smartlab diffractometer with a Co lamp (40 kV, 135 mA). The speed of acquisition was 3 deg/min at 0.02 deg/step. A small fraction of the samples (raw peat, Fe-GWTR-P3 and vanadium-treated Fe-GWTR-P3) were used for XPS and FTIR analysis. XPS was performed with a Thermo Fisher Scientific ESCALAB 250Xi using a monochromatic Al Kα source (1486.6 eV). The charge correction was done by setting the binding energy of adventitious carbon to 284.8 eV. FTIR spectra were measured in the 400-4000 cm^{-1} wavenumber region using a Bruker Vertex V80 vacuum FTIR spectrometer and OPUS program to display the recorded spectra.

2.5 Effect of pH of aqueous media and isoelectric point

The effect of pH was studied using a dosage of 2 g/L and vanadium concentration of 20 mg/L. The adsorption experiment was conducted by shaking for 24 h and following the similar procedure as that described in section 2.3. All the tests were done in duplicates. The isoelectric point (pH_{IEP}) of Fe-GWTR-P3 was measured using a dynamic light scattering instrument (Zetasizer Nano Series, Malvern Instruments Ltd., UK). An appropriate amount of Fe-GWTR-P3 was scattered in Milli-Q water. 0.1 M NaOH or HCl were used for the pH adjustment for different solutions (pH 2.06-10.33). For each pH, two repeats were prepared.

2.6 Effect of contact time

The effect of contact time was studied at a dosage of 2 g/L and an initial vanadium concentration of 20 mg/L with a pH value of 4 at room temperature. All the experiments were done in duplicates. pH

readjustment was performed for the samples with a contact time of 6 h, 24 h, 48 h and 72 h after 1 hour of shaking. The adsorption kinetics were analysed using the pseudo-first-order (PFO) equation [25], pseudo-second-order (PSO) equation [26], Elovich equation [27], intra-particle diffusion model [28] and Boyd model [29].

2.7 Vanadium sorption capacity

The Fe-GWTR-P3 was used to determine the vanadium sorption capacity. Vanadium solutions with different initial concentrations (10-130 mg/L) were prepared and the pH value was pre-adjusted to 4. Contact time (24 h) and biosorbent dosage (2 g/L), were kept constant. All the experiments were done in triplicate. Sorption capacity was calculated using the following equation:

$$q_e = \frac{(C_0 - C_e)V}{m} \quad (1)$$

where q_e is the vanadium sorption capacity (mg/g), C_0 is the initial concentration of vanadium in the solution (mg/L), C_e is the residual vanadium concentration in treated solution (mg/L), V is the volume of the solution (L), and m is the weight of the biosorbents (g).

To quantify the sorption capacity of Fe-GWTR-P3 for the removal of vanadium, three commonly used adsorption models: Langmuir [30], Freundlich [31] and Redlich-Peterson [32] were adopted to describe the experimental isotherms by non-linear regression fit.

3 Results and discussion

3.1 Dissolution of Fe-GWTR and characterization of Fe-GWTR solution

The characteristics of the-Fe-GWTR solutions are shown in Table 1. The concentration of Fe was the highest in the-Fe-GWTR solutions, in the range of 6740-6890 mg/L, followed by that of calcium,

manganese and phosphorous. Mixing time and HCl concentration did not have any significant effect on the iron concentration. It is noteworthy that Fe-GWTR solution obtained with 1 M HCl (1 h) treatment contained the smallest amount of manganese (77.2 mg/L). However, the manganese concentration of the other three Fe-GWTR solutions: 1 M HCl (6 h), 2 M HCl (1 h) and 2 M HCl (6 h) were 153, 143 and 266 mg/L, respectively, i.e. about two or three times higher than with 1 M HCl (1 h). The calcium and phosphorous concentration did not vary much for these four different Fe-GWTR solutions, with concentrations being 73.9-78.2 mg/L and 105-107 mg/L for calcium and phosphorus, respectively. As the 1 M HCl (1 h) treated Fe-GWTR solution had a high Fe concentration (6750 mg/L), and less interfering elements, this was then selected as the best dissolution conditions for Fe-GWTR used in the following experiments.

Table 1. Characteristics of Fe-GWTR solutions.

Element (mg/L)	**1M HCl (1 h)**	**1 M HCl (6 h)**	**2 M HCl (1 h)**	**2 M HCl (6 h)**
Al	1.23	1.53	0.16	1.98
As	0.15	0.14	0.16	0.17
B	<0.02	<0.02	<0.02	<0.02
Ba	14.5	16.2	15.4	17.6
Be	<0.005	<0.005	<0.005	<0.005
Ca	78.2	76.8	73.9	76.4
Cd	0.008	0.008	0.008	0.009
Co	0.28	0.57	0.50	0.95
Cr	0.035	0.036	0.033	0.037
Cu	0.24	0.24	0.22	0.25
Fe	6750	6740	6730	6890
K	11.5	8.54	10.8	9.50
Mg	7.42	7.53	7.21	7.87
Mn	77.2	153	143	266
Mo	<0.005	<0.005	<0.005	<0.005
Na	1.11	0.86	0.92	0.88
Ni	0.61	1.09	0.89	1.34
P	106	105	105	107
Pb	0.067	0.058	0.063	0.061
S	1.96	2.04	2.01	2.15
Sb	<0.015	<0.015	<0.015	<0.015
Se	<0.015	<0.015	<0.015	<0.015
Sn	0.017	0.021	0.016	0.019
Ti	0.055	0.073	0.067	0.100
V	0.059	0.055	0.066	0.074
Zn	2.02	2.16	2.09	2.33

3.2 Synthesis of the biosorbent

Since raw peat is inefficient in the uptake of vanadium from a synthetic solution (26% removal efficiency, with 2 g/L dosage at pH 5.4, initial V 20 mg/L), the modification process is a necessity. Fig. 1 shows the vanadium removal efficiency using commercial Fe ($FeCl_3 \cdot 6H_2O$) and Fe-GWTR-modified peat with three different modification pH values (3, 5 and 7). The lowest modification pH (3) was found to have the highest vanadium removal efficiency for both iron solutions, at 53% for commercial Fe-modified peat and 54% for Fe-GWTR-modified peat. The effect of pH was confirmed to be statistically significant with Fe-GWTR-modified peat at all pH values (t-test, $p < 0.05$, two-tailed) and with commercial Fe-modified peat at pH 7 (t-test, $p<0.05$, two-tailed). The difference in vanadium removal between commercial Fe-modified peat and Fe-GWTR-modified peat at pH 3 and pH 5 was not statistically significant. At pH 7, commercial Fe-modified peat removed 35.2% vanadium (st.dev. 0.75%, n=4), which was over two times higher than with Fe-GWTR-modified peat (st.dev. 0.42%, n=4), and the t-test confirmed it to be significant ($t(5)=38.8455$, $p=2.1\times10^{-7}$, two-tailed). Modification pH is a crucial variable affecting iron species loaded on biomass. Positive hydroxide species of iron dominate in acidic solution, while in the near-neutral region, insoluble iron hydroxide is formed, and therefore the binding of iron by the biomass is not so efficient. A similar result was also observed by Aryal et al. [33], in which the optimal pH for Fe(III) uptake was 3 by *Staphylococus xylosus* biomass. Zhang et al. investigated the optimal iron modification pH (5, 7 and 9) of Sphagnum moss biomass [34]. The result showed that pH 5 was the optimal modification pH and exhibited the highest phosphate removal efficiency. Therefore, as the Fe-GWTR-modified peat at pH 3 performed best in vanadium sorption, it was selected for further studies.

Fig. 1

For real wastewater treatment applications, it is also important to improve the physical properties of biosorbents, such as settling properties and mechanical stability. Fe-GWTR-P3 was found to settle

much better than natural peat (unpublished data) but worse than NaOH-treated peat [35]. Thus in practice, flocculants might be needed to further improve settling of Fe-GWTR-P3 if applied in mixing and settling systems. If applied in filter bed systems, the peat product should be granulated or mixed with another sorbent having large grain size in order to have higher hydraulic conductivity. Moreover, the iron-leaching test showed that Fe-GWTR-P3 is stable since a negligible amount of iron was leached into the solution (unpublished data). In future studies, the stability of Fe-GWTR-P3 should be confirmed with real wastewaters.

3.3 Biosorbent characterization

3.3.1 XRD analysis

Fig. 2 shows the XRD profiles of raw peat, Fe-GWTR-P3 and Comm-Fe-P3. The results revealed the presence of quartz in all three samples. The mineral characteristics of peat can be greatly affected by the region. A large presence of quartz was also observed by Romão et al. in different peat samples (collected from Itabaiana and Sao Paulo) [36]. In Romão's study [36], peat collected from Santo Amaro was amorphous. However, XRD spectra revealed mineral characteristics (presence of quartz and some clay material) in the dry ash or residue of this amorphous peat, suggesting that these minerals had been recovered by the organic matter of the peat. In this study, it was also confirmed by XRD that iron compounds introduced onto the peat existed mainly in amorphous form. In addition, the crystallinity of raw peat decreased after iron impregnation. A similar phenomenon was also found by Krishnan and Haridas [20]. However, it should be noted that after iron impregnation of peat, traces of an unidentified mineral was found in Fe-GWTR-P3 and Comm-Fe-P3.

Fig. 2

3.3.2 XPS analysis

The elemental compositions of raw peat, Fe-GWTR-P3 and vanadium-treated Fe-GWTR-P3 are shown in Table 2. Iron was successfully impregnated on the peat. The atomic percentage of oxygen increased from 21.7% to 44.0%, while the carbon percentage decreased after modification, which indicated that the chemical composition had changed during the modification process. After modification with Fe-GWTR, the silicon content slightly increased and phosphorus was introduced into the modified peat. No other impurities were found according to the analysis. A small amount of calcium was found in the raw peat. However, after modification, the peak of calcium on the survey spectrum disappeared. Vanadium was also confirmed to have attached onto the modified peat after adsorption.

Table 2. Surface composition (at.%) of raw peat, Fe-GWTR-P3 and vanadium-treated Fe-GWTR-P3 (initial concentration of vanadium=20 mg/L)

Biomass Type	Atomic percentage of the element (%)							
	C	O	N	Ca	Fe	Si	P	V
Raw peat	74.0	21.7	3.8	0.4	-	0.2	-	-
Fe-GWTR-P3	41.4	44.0	1.8	-	8.6	3.4	0.03	-
V-treated Fe-GWTR-P3	53.1	36.1	2.1	-	5.8	2.1	0.5	0.3

In the region of C 1s (Fig. 3), three components were fitted, corresponding to C1: carbon atoms bond only with carbon and/or hydrogen (C–C/C–H), centred at 284.8±0.1 eV ; C2: carbon atoms bond with a single oxygen atom and/or nitrogen (C–O/C–N), centred at 286.5±0.1 eV; C3: carbon atoms bond with two non-carbonyl oxygen atoms or a single carbonyl oxygen atom (O–C–O/C=O) and centred at 288.3±0.2 eV [37,38]. After modification, the binding energy of C3 had slightly changed and its percentage had increased from 11% to 16%, indicating that some oxygen functional groups might have been activated.

Fig. 3

The O1 s spectrum of raw peat presented only a single peak at 532.5 eV, while the O 1s spectrum of Fe-GWTR-P3 was fitted to three peaks at 532.8±0.1 eV, 531.5±0.2 eV and 530.2±0.1 eV, corresponding to C–O bonding, Fe–OH bonding and C=O bonding, and Fe–O bonding (Fig. S1) [39, 40]. The O 1s spectrum of vanadium-treated Fe-GWTR-P3 was fitted similarly; however, V–O bonding should exist at ~530 eV [41] and thus exist at a similar BE value to Fe−O bonding. The proportion of the middle component (Fe–OH, C=O) was slightly decreased and other components slightly increased, which could indicate a reaction between surface hydroxyl groups and vanadate anions. However, the change was very minor.

The shape of the Fe 2p spectra of the Fe-GWTR-P3 and vanadium-treated Fe-GWTR-P3 was almost identical (Fig. S2). The Fe $2p_{3/2}$ and Fe $2p_{1/2}$ peaks of Fe-GWTR-P3 had binding energies at 711.0 eV and 724.7 eV. However, after vanadium sorption, slight shifts of the Fe $2p_{3/2}$ and Fe $2p_{1/2}$ peaks towards a higher binding energy (711.1 eV and 724.8 eV) were observed. Similar results were also found earlier by Zhang et al. [34].

The V 2p spectra (Fig. 4) of vanadium-treated Fe-GWTR-P3 presented V $2p_{3/2}$ and V $2p_{1/2}$ peaks at 517.4 eV and 524.8 eV, which corresponds to oxidized vanadium(V) on the surface of the biosorbent [41, 42]. This suggests that on the surface, vanadium was bound by surface hydroxyl groups without a change in oxidation state change. A similar result was reported for the vanadium adsorption onto nanosized zero-valent iron [43]. It was proposed that vanadium(V) ions were bound to the outer shell of the iron sorbent via surface complexation [43].

Fig. 4

3.3.3 Surface area, pore size and pore volume

The surface physical parameters of raw peat and Fe-GWTR-P3 are shown in Table 3. In the modification, the BET surface area of Fe-GWTR-P3 increased from 22.0 m^2/g (raw peat) to 53.4

m^2/g. The nitrogen adsorption isotherms were type III isotherms, according to the IUPAC classification [44]. This type is associated with weak interaction between adsorbent and adsorbate, and there is no identifiable monolayer formation. The average pore diameter increased from 26.0 nm to 29.4 nm and the pore volume increased from 0.143 cm^3/g to 0.392 cm^3/g. The results showed that the impregnation of the iron compound changed the textural properties of raw peat.

Table 3. Surface properties of raw peat and Fe-GWTR-P3.

Materials	Raw peat	Fe-GWTR-P3
BET surface area (m^2/g)	22.0	53.4
Average pore diameter (nm)	26.0	29.4
Pore volume (cm^3/g)	0.143	0.392

3.3.4 FTIR analysis

Peat contains many functional groups such as alcohols, aldehydes, ethers, carboxylic acids, ketones and phenolic hydroxides [19]. The FTIR spectra of raw peat, Fe-GWTR-P3 and vanadium-treated Fe-GWTR-P3 showed that (Fig S3) there were no big differences between the FTIR spectra of all three samples. The presence of the –OH group is confirmed by having a band in the region of 3200-3600 cm^{-1} [45]. Two peaks exist at 2920 and 2850 cm^{-1}, ascribed to asymmetric stretching of aliphatic (C-H) [46]. The band at 1650 cm^{-1} represents carbonyl bonds (COO^-) from carboxylic acids and aromatic C=C vibrations [46]. For the vanadium-treated Fe-GWTR-P3, the peak at 3411 cm^{-1}, had shifted to 3401 cm^{-1}, which might indicate vanadium binding with the –OH group.

3.4 Effect of pH of aqueous media

The effect of pH on the sorption of vanadium by Fe-GWTR-P3 is shown in Fig. 5. Solution pH values in the range of 2.0-9.0 strongly affected vanadium sorption behaviour. Vanadium removal

efficiency was 41 % at pH 2. With an increase in pH to 4, vanadium removal efficiency reached 83 % at maximum, and then subsequently decreased to 56 % when the pH increased to 6. Afterwards, with the solution pH above the neutral value, vanadium removal efficiency decreased dramatically.

The pH_{IEP} of Fe-GWTR-P3 was found to be 5.0 (Fig. 6). Below this pH, the surface of Fe-GWTR-P3 has a positive charge and favours the uptake of anionic vanadium species. Krishnan & Haridas and Liu et al. reported that the point of zero charge (pH_{pzc}) of iron-loaded coir pith and iron-modified bamboo charcoal was observed at pH 5.8 and pH 5, respectively [20,21]; these values are very close to the pH_{IEP} of the present study.

Fig. 5

Vanadium exists in cationic form (VO_2^+) at pH 2 [47], thus the lower sorption ability may be due to the repulsion between vanadium cations and the positive charges on the surface of Fe-GWTR-P3. Above pH 3, vanadium exists as anionic vanadate species and several species may coexist at the same pH [47]. Vanadium sorption was most favourable at pH 4, which may be due to a large amount of positive charges on the surface of the sorbent. This result is also consistent with previous studies [48,49]. The decrease in sorption efficiency with increasing pH was probably due to the electrostatic repulsion between anionic vanadate species and the surface above the pH_{IEP}. At high pH values, the increasing OH^- concentration and competition with vanadium anions for the available surface sites is the most feasible explanation for the lower uptake. pH values higher than pH 9 were not even tested since it has been proved that alkaline conditions can be used for the desorption of vanadates from iron-based sorbents [50].

In summary, the optimal pH for vanadium removal can be greatly influenced by the surface charge of the sorbent material and existing vanadium species in aqueous solution. Since maximum

vanadium removal efficiency was observed at pH 4, it was selected as the optimal sorption pH and chosen as the sorption pH for further experiments in this study.

Fig. 6

3.5 Effect of contact time

Vanadium removal efficiency increased from 19.4% to 30.8% within the first hour. After 6 hours, the removal efficiency reached 50.2% and gradually increased to 76% after 24 hours. Equilibrium was achieved after 48 hours. The removal efficiency was around 84% at maximum. Reaching equilibrium was a slow process in this case, which was probably due to the amorphous or hydrous iron species loaded on the biomass surface. The pore diffusion mechanism could have a significant role, attributed to the slow equilibrium process [51,52]. Similar results have been obtained earlier for iron-based sorbents. For example, Sigdel et al. reported that alginate impregnated with hydrous iron oxide reached equilibrium for arsenic adsorption after around seven days [52]. Zhang et al. observed that phosphate sorption equilibrium was reached at about 48 hours for iron-loaded Sphagnum moss biomass, and the iron species loaded was confirmed to be two-line ferrihydrite [34].

To further investigate the adsorption kinetics, the experimental data were fitted to the non-linear pseudo-first-order (PFO), pseudo-second-order (PSO) and Elovich models. The kinetics parameters were obtained by non-linear regression (Fig. 7).

The PFO equation is expressed in the following form:

$$q_t = q_e(1 - e^{-k_1 t}) \quad (2)$$

where q_e and q_t are the amounts of adsorbate uptake per mass of adsorbent (mg/g) at equilibrium and at any time t (min), respectively; and k_1 is the pseudo-first-order rate constant (1/min). The PSO equation is expressed as:

$$q_t = \frac{q_e^2 k_2 t}{1 + k_2 q_e t} \quad (3)$$

where q_t is the adsorption capacity (mg/g) at any time *t* (min), q_e is the equilibrium adsorption capacity (mg/g) and k_2 is the pseudo-second-order rate constant (g/mg·min). The Elovich equation is expressed as:

$$q_t = \frac{1}{\beta} \ln (1 + \alpha\beta t) \quad (4)$$

where q_t is the capacity (mg/g) at any time t (min), α (mg/g × min) is the initial rate constant and β (mg/g) is the desorption constant.

The parameters obtained are presented in Table 4. The equilibrium adsorption (q_e) values obtained from pseudo-first order and pseudo-second order kinetics were close to the observed data. However, the Elovich model gave the best fit for the experimental data since the correlation coefficient (R^2) was greater than with the other two models, and the Elovich model also provided the lowest chi-squared (χ^2) value. The Elovich model is generally useful to describe chemisorption on highly heterogeneous adsorbents although it does not predict any definite mechanism [53]. Hence, these results suggest that vanadium adsorption on Fe-GWTR-P3 was mainly controlled by the chemical adsorption process.

Fig. 7

Table 4. Parameters of PFO, PSO, Elovich, intra-particle diffusion and Boyd models.

Models	Parameters	Values
Pseudo-first-order kinetic	k_1 (1/min)	0.005
	q_e (mg/g)	7.456
	R^2	0.785
	χ^2	7.381
Pseudo-second-order kinetic	k_2	0.001
	q_e (mg/g)	7.799
	R^2	0.895
	χ^2	2.211
Elovich	α (mg/g × min)	0.252

	β (mg/g)	0.827
	R^2	0.984
	χ^2	0.191
Intraparticle diffusion	$k_{i,1}$ (mg/g × $min^{½}$)	0.179
	C_1	1.390
	R_1^2	0.982
	$k_{i,2}$ (mg/g × $min^{½}$)	0.035
	C_2	5.896
	R_2^2	0.957
Boyd	R^2	0.984

The intra-particle diffusion model was used to obtain more information about the adsorption mechanism. In the adsorption process, four stages or mechanisms have been identified: bulk transport, film diffusion, intra-particle diffusion and adsorption [54]. Of all these four stages, bulk transport and adsorption are always considered negligible due to their fast occurrence.

The linearized equation of intra-particle diffusion model is described as follows [28]:

$$q_t = k_i t^{0.5} + C \quad (5)$$

where k_i (mg/g×$min^{½}$) is the intra-particle diffusion rate constant, and C (mg/g) is a constant related to the thickness of the boundary layer. When plotting q_t versus $t^{0.5}$, a straight line with a zero intercept would mean that intra-particle diffusion is the only factor controlling the adsorption process. If multiple linear regions are obtained, the adsorption process is also controlled by other mechanisms. In this study, the data could be split into two linear regions with non-zero intercepts, which indicates that intra-particle diffusion is not the only rate-controlling factor (Fig. 8). The first linear region corresponds to the film diffusion process, which means that vanadium ions are transported from the bulk solution to the surface of the adsorbent. The second linear region represents intra-particle diffusion in which vanadium ions are diffused into the pores of the adsorbent. A similar result was reported for phosphate adsorption on iron-oxide based sorbents [55].

In order to identify the actual rate-controlling step involved in the adsorption process, the Boyd model is suggested [29], which is represented as:

$$F = 1 - \frac{6}{\pi^2}\exp(-B_t) \quad (6)$$

where F represents the fraction of solute adsorbed at any time t, and B_t is a mathematical function of F. F is given by:

$$F = \frac{q}{q_e} \quad (7)$$

where q and q_e are the amount adsorbed at any time t and at equilibrium (mg/g). The equation can be rearranged as follows:

$$B_t = -0.4977 - In\,(1 - F) \quad (8)$$

The linearity of the plot B_t versus time (t) can be used to distinguish between film and intra-particle diffusion. If the Boyd plot is linear and passes through the origin, then the adsorption process is governed by intra-particle diffusion, otherwise, film diffusion governs the sorption process and can be considered as a rate-limiting step [55]. As shown in Fig. 8, the plot goes through the origin (R^2: 0.984), thus indicating that intra-particle diffusion is the rate-limiting step.

Fig. 8

3.6 Vanadium sorption capacity

Fig. 9 shows the capacity curve for vanadium sorption by Fe-GWTR-P3 at different initial vanadium concentrations (10-166 mg/L). The vanadium sorption capacity gradually increased with increasing initial vanadium concentration. When the vanadium concentration was over 80 mg/L, sorption capacity remained stable in the range of 14.8-16.3 mg/g. On the other hand, similar capacities have been reported for other anions with iron-modified biomass. Zhang et al. prepared Fe-loaded Sphagnum moss biomass and used it for phosphate removal, and the maximum capacity was around 13 mg P/g [34]. Gupta et al. used iron-chitosan flakes for removal of As(III) and As(V), and the maximum capacity was 16 mg/g and 22 mg/g, respectively [56].

Non-linear Langmuir, Freundlich and Redlich-Peterson models were used to fit the experimental data. The results are listed in Table 5.

The Langmuir isotherm model is represented mathematically as:

$$q_e = \frac{q_m b C_e}{1 + b C_e} \quad (5)$$

where q_e is the adsorbed amount of adsorbate at equilibrium (mg/g), q_m represents the maximum adsorption capacity of the adsorbent (mg/g), b is a constant related to the energy of adsorption (L/mg) and C_e is the equilibrium concentration of adsorbate in solution (mg/L).

The Freundlich model can be represented as:

$$q_e = K C_e^{1/n} \quad (6)$$

where is q_e the adsorbed amount at equilibrium (mg/g), K (L/g) and 1/n are the parameters of the Freundlich isotherm, denoting a distribution coefficient and intensity of adsorption, respectively, and C_e is the equilibrium concentration of the adsorbate in solution (mg/L).

The Redlich-Peterson model is a hybrid isotherm involving features of both the Langmuir and the Freundlich isotherms, containing three parameters in the equation. It can be described as follows:

$$q_e = \frac{A C_e}{1 + B C_e^g} \quad (7)$$

where A is the isotherm constant (L/g), B is the isotherm constant (L/mg), g is the exponent which lies between 0 and 1, and C_e is the equilibrium liquid phase concentration (mg/L).

The Redlich-Peterson model was found to provide the best fit to the experimental data since it has the highest coefficient of determination (R^2) and lowest chi-squared (χ^2) values. This model has also previously been reported to provide the best fit for other iron-impregnated biomass [34,49]. However, it should be noted that this model uses three adjustable parameters, and only two are used

in Langmuir or Freundlich. The calculated values for the maximum capacity (q_m) according to the Langmuir model are in good agreement with the experimental values, even though the fitting gave the lowest R^2 and χ^2 values.

Fig. 9

Table 5. Langmuir, Freundlich and Redlich-Peterson parameters by non-linear model for Fe-GWTR-P3.

Models	Parameters	Fe-GWTR-P3
Langmuir	q_m (mg/g)	15.622
	B (L/mg)	0.232
	R^2	0.881
	χ^2	3.816
Freundlich	K (mg/L)(L/mg)$^{1/n}$)	6.968
	n	5.292
	R^2	0.967
	χ^2	0.742
Redlich-Peterson	A (L/g)	66.050
	B (L/mg)	8.153
	g	0.846
	R^2	0.972
	χ^2	0.429

4. Conclusions

The waste material, ferric groundwater treatment residual (Fe-GWTR), could effectively be used as an iron source for iron modification of peat after dissolution with HCl. Modified peat (with 0.07 mol/L Fe) was able to remove vanadium efficiently from synthetic vanadium solution; modification under pH 3 performed best among the three different modification pH values that were tested (3, 5 and 7). Fe-GWTR was compared with commercial Fe ($FeCl_3 \cdot 6H_2O$) and confirmed to be as effective as commercial iron. Fe-GWTR is also safe to use as an iron source since no hazardous chemicals were introduced into the modified peat. Vanadium sorption was greatly affected by the pH value (maximum removal at pH 4) and contact time (equilibrium at 24-48 h). The sorption

capacity was around 16 mg/g for vanadium and data were well fitted with the Redlich Peterson isotherm. The adsorption kinetics followed the Elovich equation while the intra-particle diffusion and Boyd models revealed the influence of both film and intraparticle diffusion, with intra-particle diffusion being the slowest step. These results confirmed that waste material (Fe-GWTR) could be reused and converted into a new, effective, low-cost biosorbent for vanadium removal (or other oxyanions such as arsenic and phosphate), which is vital for sustainable development. Future studies will be focused on identifying the optimal sorption conditions for vanadium removal from real mining water as well as regeneration of sorbent material.

Acknowledgements

The research has been conducted as part of the VanProd project "Innovation for Enhanced Production of Vanadium from Waste Streams in the Nordic Region," funded by the European Union program Interreg Nord 2014−2020 and the Regional Council of Lapland.

References

[1] I. Jacukowicz-Sobala, D. Ocinski, E. Kociołek-Balawejder, Iron and aluminium oxides containing industrial wastes as adsorbents of heavy metals: application possibilities and limitations, Waste Manage. Res. 33 (2015) 612–629.

[2] P. Castaldi, M. Silvetti, G. Garau, D. Demurtas, S. Deiana, Copper(II) and lead(II) removal from aqueous solution by water treatment residues. J. Hazard. Mater. 283 (2015) 140-147.

[3] J.A. Ippolito, K.A. Barbarick, H.A. Elliott, Drinking water treatment residuals: a review of recent uses. J. Environ. Qual. 40 (2011) 1-12.

[4] T. Ahmad, K. Ahmad, M. Alam, Sustainable management of water treatment sludge through 3'R' concept. J. Clean. Prod. 124 (2016) 1-13.

[5] Y.W. Chiang, K. Ghyselbrecht, R.M. Santos, J.A. Martens, R. Swenne, V. Cappuyns, B. Meesschaert, Adsorption of multi-heavy metals onto water treatment residuals: sorption capacities and applications. Chem. Eng. J. 200-202 (2012) 405-415.

[6] A. Hovsepyan, J.C.J. Bonzongo, Aluminum drinking water treatment residuals (Al-WTRs) as sorbent for mercury: Implications for soil remediation. J. Hazard. Mater. 164 (2009) 73-80.

[7] J.A. Ippolito, K.G. Scheckel, K.A. Barbarick, Selenium adsorption to aluminium-based water treatment residuals. J. Colloid Interface Sci. 338 (2009) 48–55.

[8] J. Jiao, J. Zhao, Y. Pei, Adsorption of Co(II) from aqueous solutions by water treatment residuals. J. Environ. Sci. 52 (2017) 232-239.

[9] D. Ocinski, I. Jacukowicz-Sobala, P. Mazur, J. Raczyk, E. Kociołek-Balawejder, Water treatment residuals containing iron and manganese oxides for arsenic removal from water characterization of physicochemical properties and adsorption studies. Chem. Eng. J. 294 (2016) 210-221.

[10] Z. Li, N. Jiang, F. Wu, Z. Zhou, Experimental investigation of phosphorus adsorption capacity of the waterworks sludges from five cities in China. Ecol. Eng. 53 (2013) 165–172.

[11] I. Zohar, J.A. Ippolito, M.S. Massey, I.M. Litaor, Innovative approach for recycling phosphorous from agro-wastewaters using water treatment residuals (WTR). Chemosphere. 168 (2017) 234-243.

[12] Y.F. Zhou, R.J. Haynes, Removal of Pb(II), Cr(III) and Cr(VI) from aqueous solutions using alum-derived water treatment sludge. Water Air Soil Pollut. 215 (2011) 631-643.

[13] C. Irawan, J.C. Liu, C. Wu, Removal of boron using aluminum-based water treatment residuals (Al-WTRs). Desalination. 276 (2011) 322-327.

[14] Y.Y. Zhao, C.H. Wang, L.A. Wendling, Y.S. Pei, Feasibility of using drinking water treatment residuals as a novel chlorpyrifos adsorbent. J. Agric. Food Chem. 61 (2013) 7446-7452.

[15] C.H. Wang, Y.S. Pei, The removal of hydrogen sulfide in solution by ferric and alum water treatment residuals. Chemosphere. 88 (2012) 1178-1183.

[16] H. Soleimanifar, Y. Deng, L. Wu, D. Sarkar, Water treatment residual (WTR)-coated wood mulch for alleviation of toxic metals and phosphorus from polluted urban stormwater runoff. Chemosphere. 154 (2016) 289-292.

[17] C.H. Wang, S.J. Gao, T.X. Wang, B.H. Tian, Y.S. Pei, Effectiveness of sequential thermal and acid activation on phosphorus removal by ferric and alum water treatment residuals. Chem. Eng. J. 172 (2011) 885–891.

[18] C.H. Wang, N.N. Yuan, L.L. Bai, H.L. Jiang, Y.S. Pei, Z.S. Yan, Key factors related to drinking water treatment residue selection for adsorptive properties tuning via oxygen-limited heat treatment. Chem. Eng. J. 306 (2016) 897-907.

[19] P.A. Brown, S.A. Gill, S.J. Allen, Metal removal from wastewater using peat. Water Res. 34 (2000) 3907–3916.

[20] K.A. Krishnan, A. Haridas, Removal of phosphate from aqueous solutions and sewage using natural and surface modified coir pith. J. Hazard. Mater. 152 (2008) 527-535.

[21] X. Liu, H.Y. Ao, X. Xiong, J.G. Xiao, J.T. Liu, Arsenic removal from water by iron-modified bamboo charcoal. Water Air Soil Poll. 223 (2012) 1033–1044.

[22] C. L. Peacock, D. M. Sherman, Vanadium(V) adsorption onto goethite at pH 1.5 to 12: a surface complexation model based on ab initio molecular geometries and EXAFS spectroscopy, Geochim. Cosmochim. Acta. 68 (2004) 1723–1733.

[23] D.M. Manohar, B.F. Noeline, T.S. Anirudhan, Removal of vanadium(IV) from aqueous solutions by adsorption process with aluminum-pillared bentonite, Ind. Eng. Chem. Res. 44 (2005) 6676–6684.

[24] G.C. Li, Determination of the vanadium in aqueous solution by phosphoric acid–sodium tungstate spectrophotometry method. J. Shanxi Coal Manag. Cadre Institute, 24 (2011) 141–143. (in Chinese).

[25] S. Lagergren, About the theory of so- called adsorption of soluble substances. K. Sven. Vetensk. Handl. 24 (1898) 1−39.

[26] G. Blanchard, M. Maunaye, G. Martin, Removal of heavy metals from waters by means of natural zeolites. Water Res. 18 (1984) 1501–1507.

[27] S. Roginsky, Y.B. Zeldovich, The catalytic oxidation of carbon monoxide on manganese dioxide. Acta Phys. Chem. 1 (1934) 554.

[28] W. Weber, J. Morris, Kinetics of adsorption on carbon from solution, J. Sanit. Eng. Div. (1963) accessed March 28, 2017.

[29] G.E. Boyd, A.W. Adamson, L.S. Myers, The exchange adsorption of ions from aqueous solutions by organic zeolites. II. Kinetics1, J. Am. Chem. Soc. 69 (1947) 2836–2848.

[30] I. Langmuir, The adsorption of gases on plane surfaces of glass, mica, and platinum. J Am. Chem. Soc. 40 (1918) 1403–1461.

[31] H. Freundlich, Über die Adsorption in Lösungen. Z Phys. Chem. 57 (1906) 385-471.

[32] O. Redlich, D.L. Peterson, A useful adsorption isotherm. J. Phys. Chem. 63 (1959) 1024.

[33] M. Aryal, M. Ziagova, M. Liakopoulou-Kyriakides, Study on arsenic biosorption using Fe(III)-treated biomass of Staphylococcus xylosus. Chem. Eng. J. 162 (2010) 178-185.

[34] R.C. Zhang, T. Leiviskä, S. Taskila, J. Tanskanen, Iron-loaded Sphagnum moss extract residue for phosphate removal. J. Environ. Manage. 218 (2018) 271-279.

[35] T. Leiviskä, M.K. Khalid, H. Gogoi, J. Tanskanen, Enhancing peat metal sorption and settling characteristics. Ecotoxicol. Environ. Saf. 148 (2018) 346-351.

[36] L.P.C. Romão, J.R. Lead, J.C. Rocha, L.C. Oliveira, A.H. Rosa, A.G.R. Mendonça, A.S. Ribeiro, Structure and properties of Brazilian peat: analysis by spectroscopy and microscopy. J. Braz. Chem. Soc. 14 (2007) 714–720.

[37] S.R. Kelemen, M. Afeworki, M.L. Gorbaty, P.J. Kwiatek, M. Sansone, C.C. Walters, Thermal transformations of nitrogen and sulfur forms in peat related to coalification. Energy Fuels. 20 (2006) 635-652.

[38] C.M. Popescu, C.M. Tibirna, C. Vasile, XPS characterization of naturally aged wood. Appl. Surf. Sci. 256 (2009) 1355-1360.

[39] H. Ardelean, S. Petit, P. Laurens, P. Marcus, F. Arefi-Khonsari, Effects of different laser and plasma treatments on the interface and adherence between evaporated aluminium and polyethylene terephthalate films: X-ray photoemission, and adhesion studies. Appl. Surf. Sci. 243 (2005) 304-318.

[40] G. Cui, M. Liu, Y. Chen, W. Zhang, J. Zhao, Synthesis of a ferric hydroxide-coated cellulose nanofiber hybrid for effective removal of phosphate from wastewater. Carbohydr. Polym. 154 (2016) 40-47.

[41] F. Ureña-Begara, A. Crunteanu, J.P. Raskin, Raman and XPS characterization of vanadium oxide thin films with temperature, Appl. Surf. Sci. 403 (2017) 717–727.

[42] G. Silversmit, D. Depla, H. Poelman, G.B. Marin, R. De Gryse, Determination of the V2p XPS binding energies for different vanadium oxidation states (V^{5+} to V^{0+}). J. Electron. Spectrosc. Relat. Phenom. 135 (2004) 167–175.

[43] A.E. Yayayürük, O. Yayayürük, Adsorptive performance of nanosized zero-valent iron for V(V) removal from aqueous solutions. J. Chem. Technol. Biotechnol. 92 (2017)1891-1898.

[44] M. Thommes, K. Kaneko, A.V. Neimark, J.P. Olivier, F. Rodriguez-Reinoso, J. Rouquerol, K.S.W. Sing, Physisorption of gases, with special reference to the evaluation of surface area and pore size distribution (IUPAC Technical Report). Pure Appl. Chem. 87 (2015) 1051-1069.

[45] D.H. William, I. Fleming, Spectroscopic Methods in Organic Chemistry, fifth ed. McGraw-Hill, London. (1995) ISBN 0-07-709147-7.

[46] C. Cocozza, V. D'Orazio, T.M. Miano, W. Shotyk, Characterization of solid and aqueous phases of a peat bog profile using molecular fluorescence spectroscopy, ESR and FT-IR, and comparison with physical properties. Org. Geochem. 34 (2003) 49–60.

[47] J. Guzman, I. Saucedo, R. Navarro, J. Revilla and E. Guibal, Langmuir, 18 (2002) 1567–1573.

[48] T.S. Anirudhan, S. Jalajamony, L. Divya, Efficiency of amine-modified poly(glycidyl methacrylate)-grafted cellulose in the removal and recovery of vanadium(V) from aqueous solutions. Ind. Eng. Chem. Res. 48 (2009) 2118-2124.

[49] L. Zhang, X. Liu, W. Xia, W. Zhang, Preparation and characterization of chitosan-zirconium(IV) composite for adsorption of vanadium(V). Int. J. Biol. Macromol. 64 (2014) 155-161.

[50] M.K. Khalid, T. Leiviskä, J. Tanskanen, Properties of vanadium-loaded iron sorbent after alkali regeneration. Water Sci. Technol. 76 (2017) 2672-2679.

[51] P.J. Swedlund, H. Holtkamp, Y. Song, C.J. Daughney, Arsenate-ferrihydrite systems from minutes to months: a macroscopic and IR spectroscopic study of an elusive equilibrium. Environ. Sci. Technol. 48 (2014) 2759-2765.

[52] A. Sigdel, J. Park, H. Kwak, P.K. Park, Arsenic removal from aqueous solutions by adsorption onto hydrous iron oxide-impregnated alginate beads. J. Ind. Eng.Chem. 35 (2016) 277-286.

[53] H. Chen, A.Q. Wang, Adsorption characteristics of Cu(II) from aqueous solution onto poly(acrylamide)/attapulgite composite, J. Hazard. Mater. 165 (2009) 223–231.

[54] H.N. Tran, S.J. You, A. Hosseini-Bandegharaei, H.P. Chao, Mistakes and inconsistencies regarding adsorption of contaminants from aqueous solutions: a critical review, Water Res. 120 (2017) 88–116.

[55] J. Lalley, C. Han, X. Li, D.D. Dionysiou, M.N. Nadagouda, Phosphate adsorption using modified iron oxide-based sorbents in lake water: kinetics, equilibrium, and column tests, Chem. Eng. J. 284 (2016) 1386–1396.

[56] A. Gupta, V.S. Chauhan, N. Sankararamakrishnan, Preparation and evaluation of iron-chitosan composites for removal of As(III) and As(V) from arsenic contaminated real life groundwater. Water Res. 43 (15) (2009) 3862-3870.

[57] P. Lodeiro, S.M. Kwan, J.T. Perez, L.F. Gonzalez, C. Gerente, Y. Andres, G. McKay, Novel Fe loaded activated carbons with tailored properties for As(V) removal: adsorption study correlated with carbon surface chemistry. Chem. Eng. J. 215 (2013) 105-112.

FIGURE CAPTIONS:

Fig. 1. Effect of modification pH on vanadium sorption (biosorbent dose 2 g/L; contact time 24 h; sorption solution pH 6; initial vanadium concentration 20 mg V/L; temperature 20 ± 3 ˚C; error bars represent the standard deviation of four repeats: two products made in the same conditions and two shaking tests for each product).

Fig. 2. X-ray diffraction profiles of (a) raw peat, (b) Fe-GWTR-P3, and (c) Comm-Fe-P3.

Fig. 3. C 1s spectra of (a) raw peat; (b) Fe-GWTR-P3; (c) vanadium-treated Fe-GWTR-P3.

Fig. 4. V 2p spectra of vanadium-treated Fe-GWTR-P3.

Fig. 5. Effect of pH on vanadium removal by Fe-GWTR-P3 (biosorbent dose 2 g/L; contact time 24 h; initial vanadium concentration 20 mg V/L; temperature 20 ± 3 ˚C; error bars represent the range of duplicate data).

Fig. 6. Determination of the pH of the zero point of charge for Fe-GWTR-P3 (error bars represent the range of duplicate data).

Fig. 7. Pseudo-first-order, pseudo-second-order and Elovich kinetics by non-linear model and experimental kinetics for the sorption of vanadium onto Fe-GWTR-P3 (biosorbent dose 2 g/L; sorption solution pH 4; initial vanadium concentration 20 mg V/L; temperature 20 ± 3 ˚C; error bars represent the range of duplicate data).

Fig. 8. Intra-particle diffusion model (a) and Boyd model (b) for vanadium adsorption onto Fe-GWTR-P3 (biosorbent dose 2 g/L; sorption solution pH 4; initial vanadium concentration 20 mg V/L; temperature 20 ± 3 ˚C; error bars represent the range of duplicate data).

Fig. 9. Langmuir, Freundlich and Redlich-Peterson isotherms by nonlinear models and the experimental data for the sorption of vanadium onto Fe-GWTR-P3 (biosorbent dose 2 g/L; contact time 24h; sorption solution pH 4; temperature 20 ± 3 ˚C; error bars represent the deviation of three repeats).

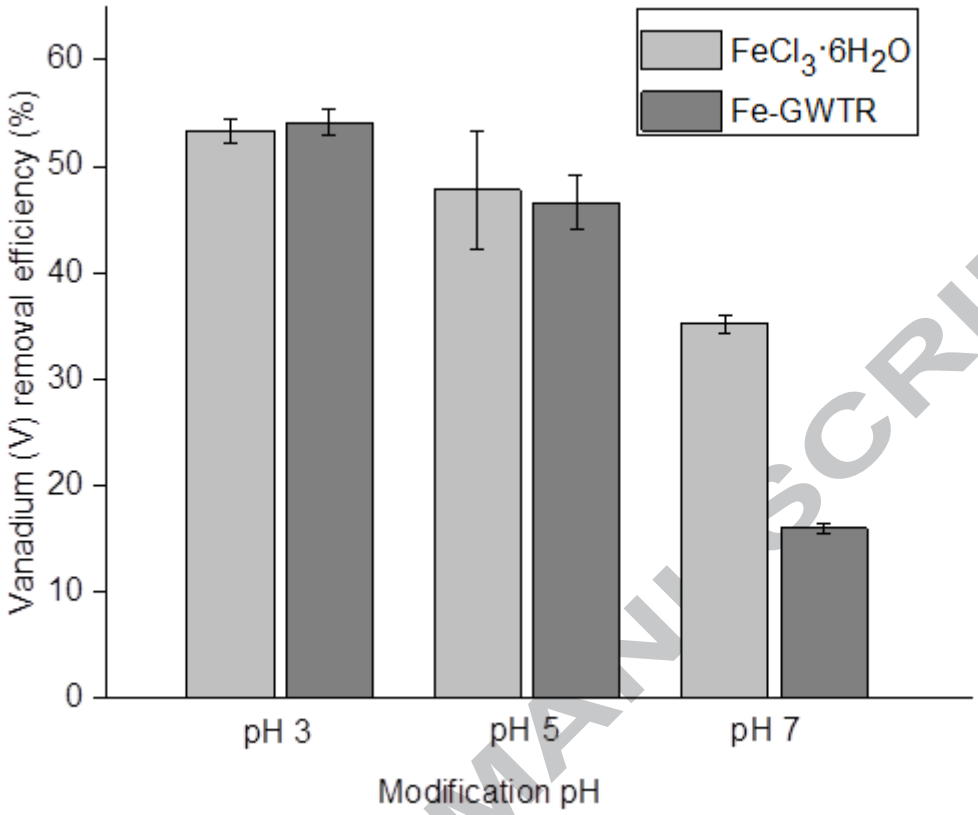
FeCl3·6H2O
Fe-GWTR
Vanadium (V) removal efficiency (%)
0
10
20
30
40
50
60
pH 3
pH 5
pH 7
Modification pH

Fig. 1

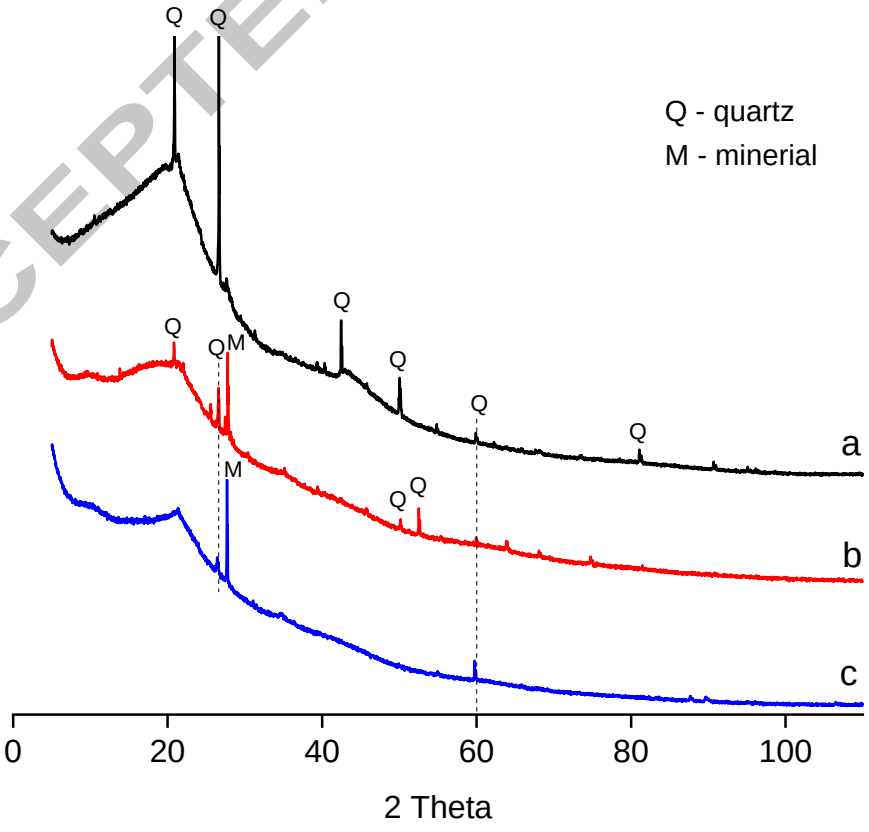
Q - quartz
M - minerial
Q
M
a
b
c
0
20
40
60
80
100
2 Theta

Fig. 2

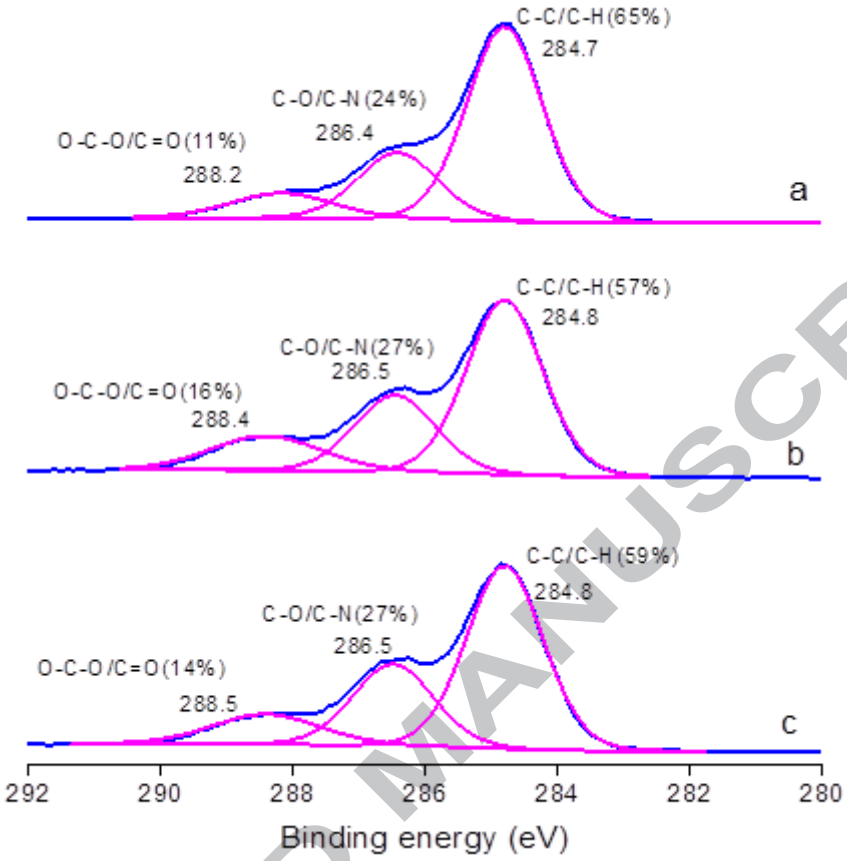

Fig. 3

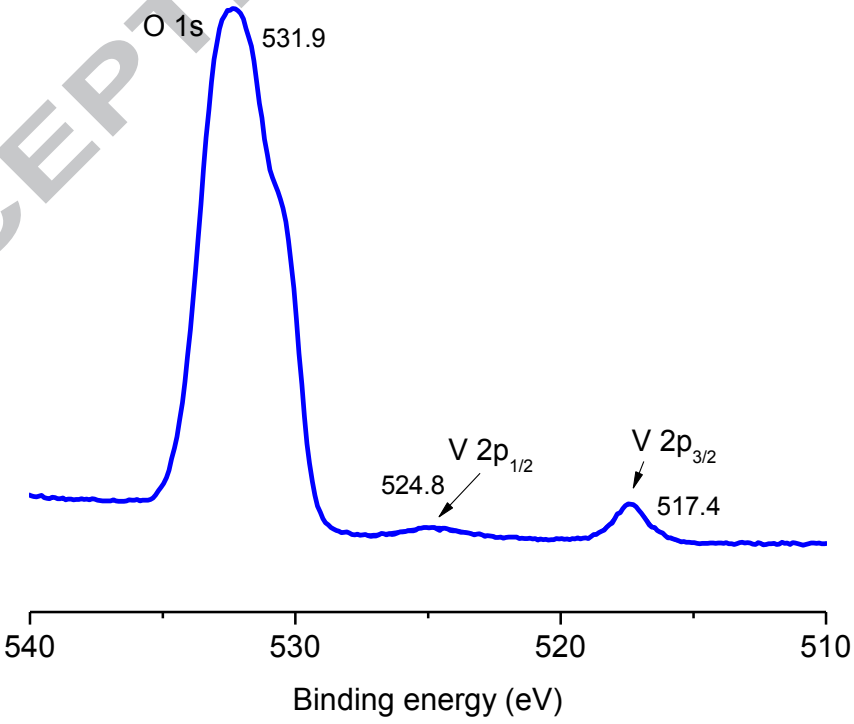

Fig. 4

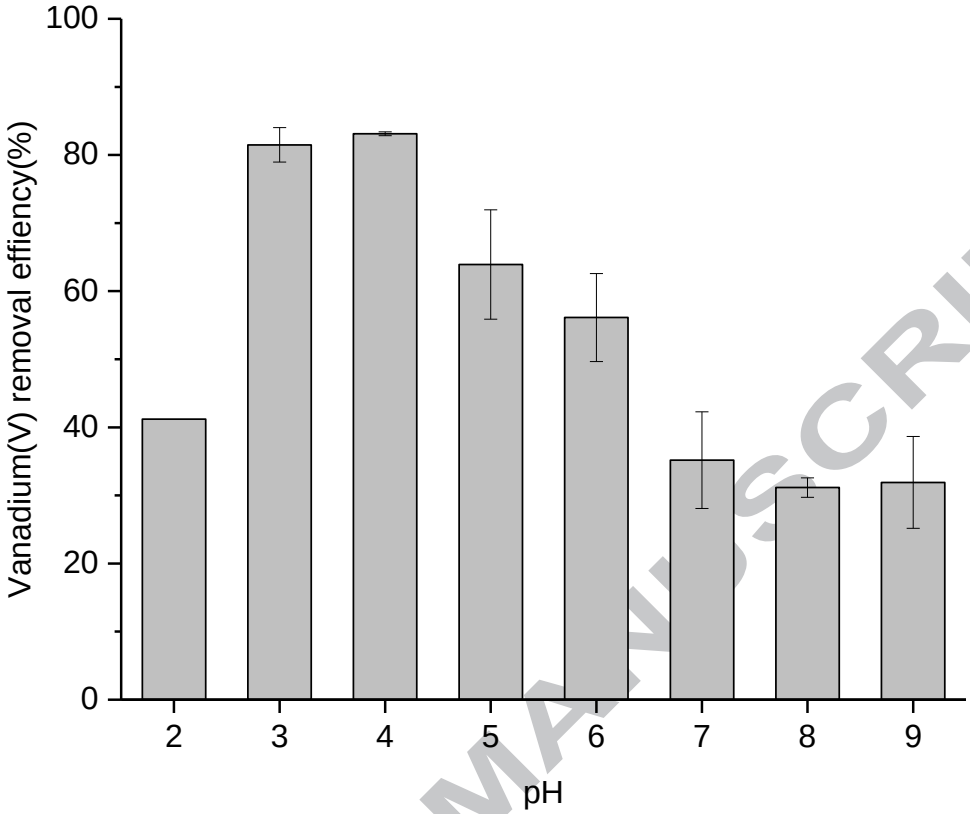

Fig. 5

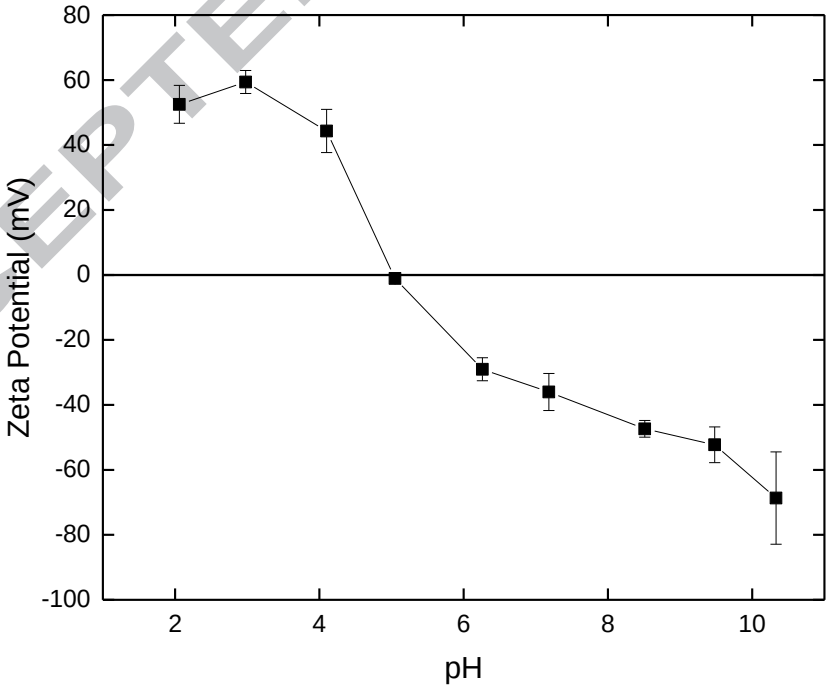

Fig. 6

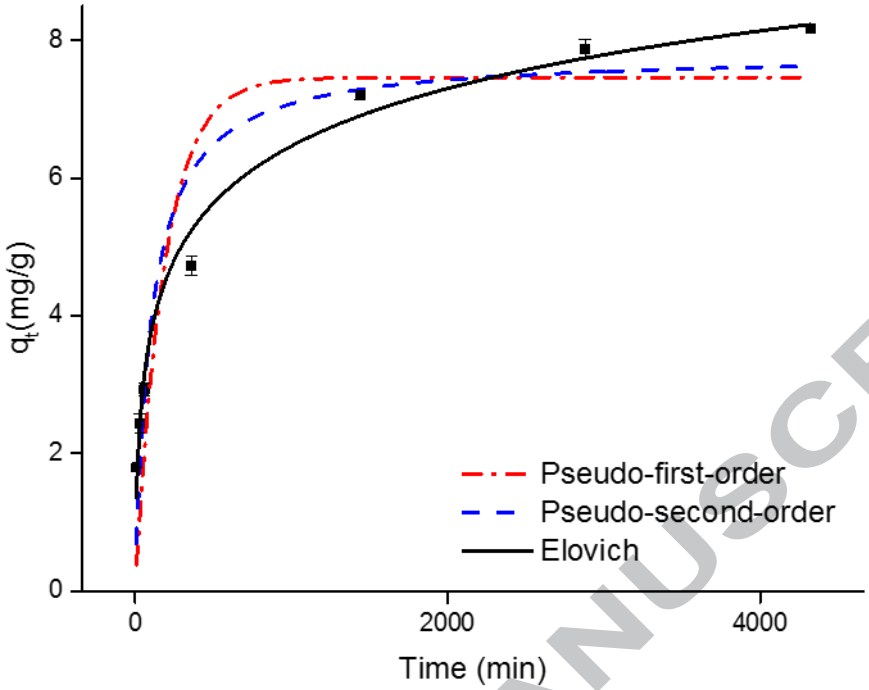

Fig. 7

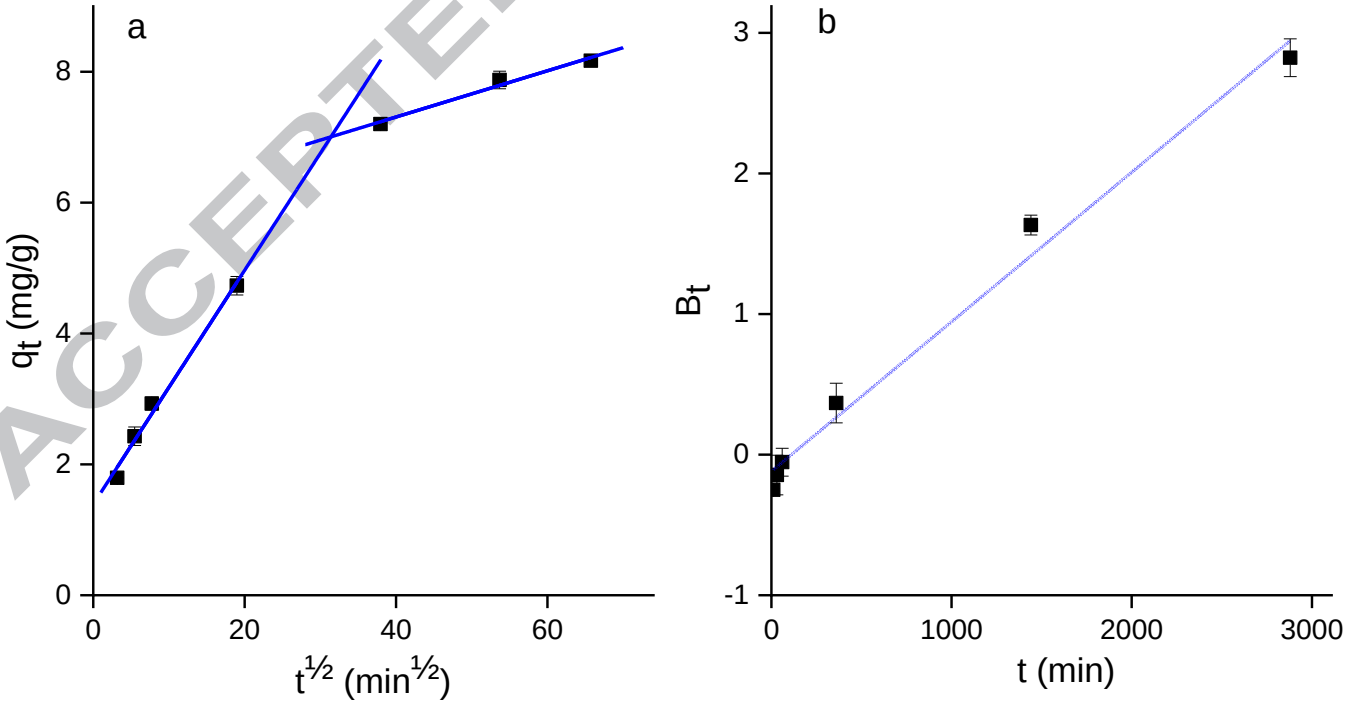

Fig. 8

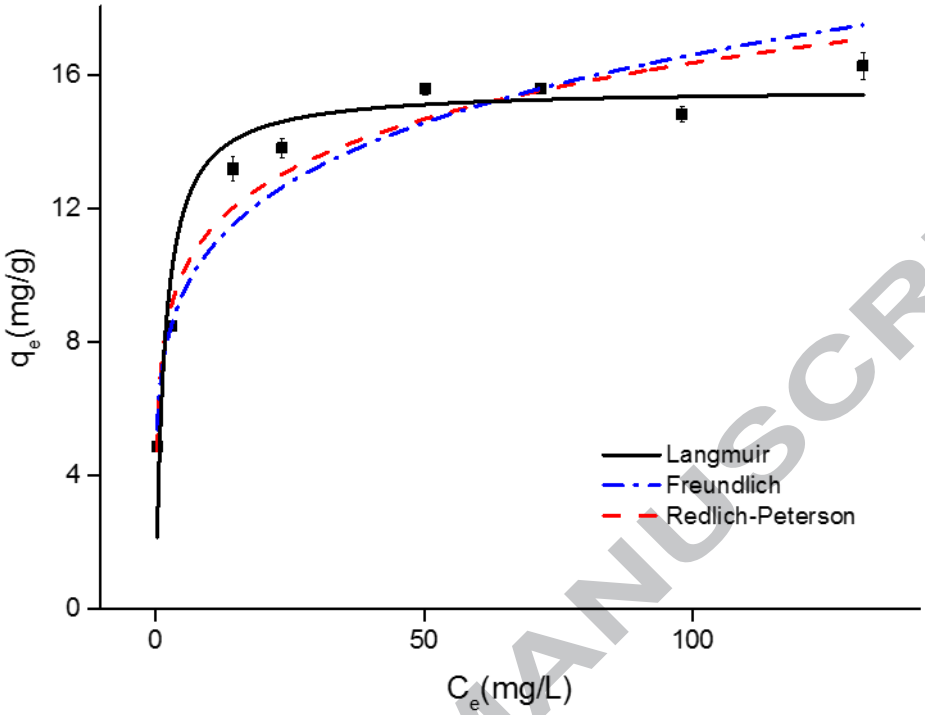

Fig. 9

- Fe-GWTR is as efficient as $FeCl_3 \cdot 6H_2O$ as an iron source for Fe modification
- No hazardous chemicals from Fe-GWTR introduced into modified biomass
- Maximum capacity for vanadium is 16 mg/g